Genomic diversity of novel strains of mammalian gut microbiome derived *Clostridium* XIVa strains is driven by mobile genetic element acquisition

Maya T. Kamat[a$], Michael J. Ormsby[a,b$], Suzanne Humphrey[a], Shivendra Dixit[a], Katja Thümmler[a], Craig Lapsley[a], Kathryn Crouch[a], Caitlin Jukes[a], Heather Hulme[a,c], Richard Burchmore[a], Lynsey M. Meikle[a], Leighton Pritchard[c,*] and Daniel M. Wall[a,*]

[a]*School of Infection and Immunity, College of Medical, Veterinary and Life Sciences, Sir Graeme Davies Building, University of Glasgow, Glasgow G12 8TA, United Kingdom*

[b]*Biological and Environmental Sciences, Faculty of Natural Sciences, University of Stirling, Stirling, FK9 4LA, United Kingdom*

[c]*Strathclyde Institute of Pharmacy & Biomedical Sciences, Strathclyde University, Glasgow G4 ORE, United Kingdom*

[$]*Contributed equally to the work*

**Corresponding author email addresses: Donal.Wall@glasgow.ac.uk; Leighton.Pritchard@strath.ac.uk*

Abstract

Despite advances in sequencing technologies that enable a greater understanding of mammalian gut microbiome composition, our ability to determine a role for individual strains is hampered by our inability to isolate, culture and study such microbes. Here we describe highly unusual *Clostridium* XIVa group strains isolated from the murine gut. Genome sequencing indicates that these strains, *Clostridium symbiosum* LM19B and LM19R and *Clostridium clostridioforme* LM41 and LM42, have significantly larger genomes than most closely related strains. Genomic evidence indicates that the isolated LM41 and LM42 strains diverge from most other *Clostridium* XIVa strains and supports reassignment of these groups at genus-level. We attribute increased *C. clostridioforme* LM41 and LM42 genome size to acquisition of mobile genetic elements including dozens of prophages, integrative elements, putative group II introns and numerous transposons including 29 identical copies of the IS66 transposase, and a very large 192 Kb plasmid. antiSmash analysis determines a greater number of biosynthetic gene clusters within LM41 and LM42 than in related strains, encoding a diverse array of potential novel antimicrobial compounds. Together these strains highlight the potential untapped microbial diversity that remains to be discovered within the gut microbiome and indicate that, despite our ability to get a top down view of microbial diversity, we remain significantly blinded to microbe capabilities at the strain level.

Introduction

The intestinal microbiome is now recognized as playing an important role in the maintenance of human health, providing protection from invading pathogens and potentially contributing to a variety of diseases when disrupted [1–6]. While significant progress has been made in understanding alterations to the human gut microbiome across a range of diseases, identification of a defined mechanistic role for the microbiome in many of these diseases has yet to be elucidated. However, significant and reproducible alterations in the gut microbiome associated with many diseases have added further weight to the suggestion that bidirectional communication between the gut and various organs, including the brain, may contribute to specific conditions. Microbiome-derived metabolites and microbe-modulated host neurotransmitters are known to cross the blood-brain barrier [5, 7–10], and *Lachnospiraceae*-derived metabolites localize to the white matter of the murine brain and inhibit energy production in white matter cells when tested *ex vivo* [9]. As microbiome science progresses a greater understanding of the capabilities of the gut microbiome, and not just its composition, is becoming increasingly the focus.

Increased presence of certain *Lachnospiraceae* in the human gut is associated with weight gain and antibiotic use [11–13]. *Clostridium* (a member of the *Lachnospiraceae* family) is a key genus within the gut microbiome known to modulate host immune and metabolic processes [14–16]. The current taxonomic classification of the genus *Clostridium* comprises approximately 150 metabolically diverse species of anaerobes. The genus is almost ubiquitous in anoxic habitats where organic compounds are present, such as soils, aquatic sediments, and the intestinal tracts of animals and humans [17]. Genome sizes differ significantly among *Clostridia* with the larger genomes of certain *Lachnospiraceae* species such as *Clostridium clostridioforme* (more recently reclassified as *Enterocloster clostridioformis*) and *Clostridium bolteae* hypothesized to contain genomic features that underlie their ability to colonize the disrupted intestinal microbiome, likely by means of increased metabolic capabilities [11, 12, 18]. *C. bolteae* populations are known to significantly increase in number post-antibiotic treatment in the human gut, and this increase can persist for 180 days post-treatment [11, 12]. *Lachnospiraceae* species such as *C. clostridioforme* are also significantly increased in the gut microbiome of patients with type 2 diabetes mellitus and autism spectrum disorders, and are discriminatory of the low gene content in the intestine associated with obesity, while increases in *C. symbiosum* numbers have been associated with colorectal cancer [13, 19–22]. Given their links to metabolic disease, dietary changes, cancer and antibiotic use, the increased presence of these strains of *Lachnospiraceae* in the intestine under certain conditions has been taken to be indicative of a Western lifestyle.

Alteration of the human gut microbiome occurs through multiple mechanisms including dietary selection, as evidenced by the changing gut microbiome in infants as they progress to adulthood, and also through insults such as environmental changes, various disease states, and medical interventions such as the use of antibiotics [11, 12, 23–25]. These can result in distinctive shifts in human gut microbiota profiles with specific families or species of bacteria increasing or decreasing in number in response to change. Why some microbes succeed and proliferate over others under such circumstances is incompletely understood, but hypotheses include increased antibiotic resistance and metabolic capabilities in those strains that successfully respond to change [11, 12, 23]. Here we characterize in detail recently-isolated strains of *C. clostridioforme* and *C. symbiosum,* two species that proliferate in response to perturbations of the gut microbiota as well as producing novel metabolites of significance for mammalian health [9]. We undertook comparative genomic and phylogenetic analysis of these poorly characterized species. The *C. clostridioforme* and *C. symbiosum* strains isolated and sequenced here have significantly larger genomes with a significantly increased number and diversity of mobile genetic elements (MGEs) in comparison with closely related strains. Our findings indicate that the *C. clostridioforme* strains isolated here have an unusual ability to harbour, and likely also acquire, MGEs with their increased genome size largely attributable to these elements.

Materials and methods

Bacterial strains and growth conditions.

Bacterial strains were isolated by removal of the whole intestine from mice and culturing the gut contents on fastidious anaerobe broth (FAB) agar (Neogen, UK) at 37°C under anaerobic conditions. The sequenced isolates were isolated from a Fragile X syndrome mouse (*Fmr1*$^{-/y}$) colony (*Fmr1* KO mouse) [26]. Selected colonies were grown on solid FAB media and 16S rDNA PCR was carried out as previously described [9] enabling the establishment of putative identities based on 16S rDNA analysis. In preparation for sequencing all strains were grown in liquid cultures prepared by inoculating a single isolated colony into FAB (Neogen, UK) and growing at 37°C without shaking in an anaerobic cabinet.

Genome sequencing

Genomes of the four strains, putatively identified by 16S rDNA sequencing as *Clostridium symbiosum* (strains LM19B and LM19R) and *Clostridium clostridioforme* (strains LM41A and LM42D), were obtained using two sequencing technologies. First, bacterial lawns were generated from single colonies. Genomic DNA was extracted using Purelink Genomic DNA kit (Invitrogen K182001). Widened pipette tips were used to maintain higher molecular weight DNA. Additionally, the protocol from Invitrogen was altered as to not include any vortexing but instead shaking to prevent excess DNA shearing. The final elution step was carried out in distilled water rather than the kit elution buffer to allow better downstream processing and the samples sent to MicrobesNG (Birmingham University, UK) for Illumina and MinION hybrid sequencing. The draft genomes have been deposited at GenBank in BioProject PRJNA936716; and under BioSample numbers; LM19B; SAMN33749590, LM19R; SAMN33749591, LM41; SAMN33749588 and LM42; SAMN33749589.

Genomic analysis

Genome analysis was conducted using CLC genomics workbench (v.7.0.1) and comparative genomic analysis performed through OrthoFinder v2.5.2, Prodigal v2.6.3 and Roary v3.12.0 [22–24]. Open reading frames were found using Glimmer3.02 [27]. Pairwise average nucleotide identities were calculated for the four sequenced isolates *Clostridium symbiosum* LM19B, *Clostridium symbiosum* LM19R, *Clostridium clostridioforme* LM41A and *Clostridium clostridioforme* LM42D, alongside 162 *Lachnoclostridium* (NCBI:txid1506553) genomes downloaded from NCBI on 13th December 2019. Genomes were downloaded with, and ANIm calculated using, pyani v0.3.0a1 [27]. AntiSMASH (v4.1.0) was used to analyse secondary metabolite production [25]. Phage detection in the bacterial strains was undertaken using Phaster [26]. Transposons were detected with Tn Central [28] and integrative elements were detected using ICEfinder v1.0 [29]. Plasmids in *C. clostridioforme* strains LM41 and LM42 were annotated using RAST and ORF identities were then manually curated using BLAST v2.12.0 [30, 31].

Results

Increased genome size in *C. clostridioforme* strains LM41 and LM42

The *C. clostridioforme* strains isolated and sequenced here, LM41 and LM42, at 7.78 Mb had larger genomes than those of all other *C. clostridioforme* and *Clostridium* XIV*a* strains obtained from NCBI (range of genome size 5.4 – 6.7 Mb) (Table 1). The closest strain in size was *C. clostridioforme* YL32 which, at 7.2 Mb, was only 0.6 Mb smaller and also grouped more closely phylogenetically with LM41 and LM42 (Fig. 1). Both *C. symbiosum* strains, LM19B (5.29 Mb) and LM19R (5.29 Mb), were comparable in size to that of a *C. symbiosum* LT0011 reference isolate. *C. clostridioforme* LM41 and LM42 had the lowest GC content of all sequenced *C. clostridioforme* strains while *C. symbiosum* LM19B and LM19R had comparable GC content to other *C. symbiosum* strains (Table 1).

Whole-genome average nucleotide identity (ANIm) analysis was conducted for the 4 isolated strains and 162 *Lachnoclostridium* genomes obtained from GenBank, and ten additional isolates using pyani v0.3.0a1 [27]. The resulting plot indicated more than 20 groups of sequenced isolates that, in pairwise alignments, mutually share at least 50% of their genomic material with each other but share only a small proportion (0-10%) of their sequenced genome with any other group (Fig. 2). In other families, these groupings are seen to coincide with recognised genus-level taxonomic divisions, implying that the existing *Lachnoclostridium* genus classification may benefit from genome-informed taxonomy revision.

The largest such grouping (group 1) contains 48 genome sequences, including sequenced isolates *C. clostridioforme* LM41, LM42, 90A7, CM201 and YL32 and *C. bolteae* BAA613, and all NCBI-downloaded isolates assigned as *C. bolteae* or *C. clostridioforme*. The next-largest grouping (group 2) contains 17 genome sequences, including *C. symbiosum* isolates LM19B, LM19R, LT0011, and C14940, and all NCBI-downloaded isolates assigned as *C. symbiosum*. We refer to these as the (1) *C. bolteae*/*C. clostridioforme* and (2) *C. symbiosum* groups respectively but note that this genomic evidence supports nomenclature reassignment of these groups at genus-level (Fig. 2).

All genomes in the *C. symbiosum* grouping share at least 77% of their total genomic sequence in homologous alignment with other members of the grouping. The *C. symbiosum* LM19B and LM19R genomes share nearly 100% of their genomes with each other in this way, but only 77-83% with the other *C. symbiosum* genomes, indicating that approximately 20% of the LM19B and LM19R genomes are unique to those strains, among the sequenced isolates.

The *C. bolteae*/*C. clostridioforme* grouping is divisible into four major subgroups. The collection of *C. bolteae* isolates each share at least 73% of their genome in homologous alignment, but no more than 57% of their genome with the other members of the larger grouping. Similarly, the *C. clostridioforme* isolates share at least 62% (and usually at least 75% of their genomes in homologous alignment with other members of the *C. clostridioforme* group), but (mostly) no more than 66% with any other member of the larger grouping. The remaining groups are complex, and include the *C. clostridioforme* grouping of isolates YL32, LM41 and LM42. The *C. clostridioforme* set share at least 67% of their genomes with these three isolates; however, YL32, LM41 and LM42 share no more than 60% of their genomes with any *C. clostridioforme* genome. This asymmetry indicates that a considerable amount of material that is not homologous to the other *Clostridia* in this study has been incorporated into the genomes of these three isolates. Specifically, the alignments of LM41 and LM42 share 7.6 Mbp of genome sequence with each other, 4.7 Mbp with YL32, but no more than 4.5 Mbp with other *C. clostridioforme*. Likewise, YL32 (genome size: 7.2 Mbp) alignments share no more than 4.3 Mbp with any other *C. clostridioforme*.

ANIm analysis indicates that *C. symbiosum* (minimum 99% identity), *C. bolteae* (minimum 97% identity) and *C. clostridioforme* (minimum 98% identity) constitute distinct species groups and belong to the same genus (Fig. 2). Some isolates appear to have been assigned to an incorrect species (e.g., *C. clostridioforme* AM07-19 and 90A7, which we identify as *C. bolteae*), and two isolates (*C. bolteae* W0P9.022 and *C. clostridioforme* AGR2 157) appear to be the single examples of distinct novel species; W0P9.022 shares no more than 7.5% of homologous genome sequence with any of the other isolates in the figure and so should be considered to belong to a distinct genus.

Despite the additional genomic material noted above, homologous alignment with the other members of their groups unambiguously places isolates LM41 and LM42 as *C. clostridioforme* and LM19B and LM19R as *C. symbiosum*, taxonomically. Reannotation of the 55 *C. bolteae*, *C. clostridioforme*, and *C. symbiosum* genomes identified above (excluding W0P9.022) using Prokka, followed by pangenome analyses with Roary, suggests core genome sizes consistent with other bacterial species for *C. clostridioforme* (1898 genes), *C. bolteae* (3085 genes) and *C. symbiosum* (2936 genes) (Figure 3, Table 2 and Supplementary Figures 1-3). In *C. symbiosum* 47% of total genes were determined to be “cloud” genes (5125 of 10887 genes) while in *C. bolteae* this was 50% (7698 of 15420 genes). In *C. clostridioforme* however there was a significant increase in size of the accessory genome 55% of genes, of the total of 25402, identified as cloud genes.

Increased phage carriage in *C. clostridioforme* LM41 and LM42

Given the relative increase in size of the accessory genome of *C. clostridioforme* isolates LM41 and LM42 in comparison to other *C. clostridioforme* strains, we sought to determine whether acquisition of new genetic material through mobile genetic elements (MGEs) could account for at least some of the increase in genome size. Initially, using the phage search tool Phaster [32], a significantly increased number of putative prophages were predicted in LM41 and LM42 in comparison to other *C. clostridioforme* strains (Table 3). These putative prophages comprised over 12% of the total genome in both these strains, more than double the genetic material ascribed to predicted prophages in any other *C. clostridioforme* strain, except for the most closely related strain YL32 in which 8.6% of its genome was determined to be of likely prophage origin. Predicted prophage material made up between 1.9 and 5.5 % of all other *C. clostridioforme* strain genomes, with all these strains also having significantly smaller genomes than *C. clostridioforme* LM41, LM42 and YL32 (Table 3). While many predicted prophages were common to both *C. clostridioforme* LM41 and LM42, a number of these differed between the strains (Table S1).

For *C. symbiosum* strains LM19B and LM19R a similar evolution towards increased prophage tolerance was noted. These strains, with significantly smaller genomes than *C. clostridioforme* (5.29 Mb versus 7.78 Mb respectively), were identified as each having 8 prophages, comprising just under 5% of the total genome (Table 3). This was a significant increase in predicted phage number compared to the other *C. symbiosum* strains, which all have fewer prophages, except for WAL-14163 which had 12 predicted prophages that make up over 7% of its total genetic material. *C. bolteae* isolates had a range of phage numbers comprising anywhere from 0.1 to 7 % of their total genome across the 18 sequenced strains. However, the majority had few, if any, predicted intact prophages, and none had greater than 4% of their genome annotated as being phage derived. While 29 and 28 prophages were predicted in *C. clostridioforme* LM41 and LM42 respectively, these are likely not all functional and will need to be investigated further.

With the large number of predicted prophages in *C. clostridioforme* strains LM41 and LM42, and the comparable genome sizes between the strains (7.78 Mb for each), it was hypothesized that these strains derive from a recent common ancestor. However further examination of the prophage content of each strain indicated that, of the prophages present in each, only 23 were common to both *C. clostridioforme* LM41 and LM42 with each having at least 5 unique predicted prophage elements (Supplementary Table 1). Additionally, many prophages were distributed and orientated differently in each isolate. In the case of *C. symbiosum* strains LM19B and LM19R no phage was found that was predicted to be common to both strains (data not shown).

Increased presence of MGEs other than phage in *C. clostridioforme* LM41 and LM42

C. clostridioforme LM41 and LM42 both carried an identical large plasmid of 192,394 bp in size (pCclLM41_1 and pCclLM42_1 respectively). The plasmid had a significantly lower GC content than either genome, at 44.6% GC (versus 47.8% for each genome). It was highly stable, and despite attempts to cure *C. clostridioforme* LM41 of the plasmid over 12 weeks through repeated subculturing in nutrient rich media it was retained. No single nucleotide polymorphisms (SNPs) appeared over this time (data not shown). The plasmid contains a number of intriguing predicted ORFs, in the context of intestinal colonisation. The first predicted protein was very large, 3824 amino acids in length, and bears significant homology to the approximately 500 amino acid SpaA isopeptide forming pilin-like protein from *Corynebacterium diphtheriae* [33]. However, rather than encoding a pilin monomer, the SpaA motif was identified as repeating 15 times within this protein. SpaA-derived pilins play an important role in *C. diphtheriae* virulence, enabling attachment to specific tissues, suggesting that this large protein possibly encodes a protein with a similar contribution to adhesion in *C. clostridioforme* [33]. Additionally, a BGC containing a large non-ribosomal peptide synthetase (NRPS) of 2759 amino acids was identified in the plasmid next to a Sec system translocase. This NRPS is predicted by antiSmash to encode for an enniatin-like antimicrobial.

The larger genome size and accessory genomes of *C. clostridioforme* LM41 and LM42, in comparison to other strains of *C. clostridioforme*, motivated detailed examination of these genomes for the presence of MGEs other than prophages and plasmids, that may contribute to the genome size difference. We found evidence for the abundant presence of multiple types of MGEs. Using the ICEfinder tool to search the *C. clostridioforme* LM41 genome we identified seven putative integrative and conjugative elements (ICE), each with an associated type 4 secretion system (T4SS), and five putative integrative and mobilizable elements (IME), alongside what is termed an *Agrobacterium tumefaciens* integrative and conjugative element (AICE) (Table 4) [29]. A more diverse array of ICEs and IMEs was identified in *C. clostridioforme* LM42: 17 in total including eight putative ICEs with their own T4SS and nine IMEs. These elements differed significantly in their size and distribution between LM41 and LM42. *C. symbiosum* LM19B contained two putative IMEs and a single ICE while *C. symbiosum* LM19R had three putative IMEs and two putative ICEs, but there was low sequence identity between the regions from both *C. symbiosum* LM19B and LM19R, and a significant size discrepancy between them (Table 4). IS66 transposases were predicted in a number of putative phage regions identified by Phaster in the genomes of *C. clostridioforme* LM41 and LM42, potentially leading to their misidentification as phage elements [32]. Further examination of the genome of *C. clostridioforme* LM41 indicated the presence of 27 identical copies of the IS66 transposase (each at 1623 bp and 100% nucleotide identity), alongside two further copies that were either partial or not identical. Additionally, a further two identical copies of IS66 were identified on the plasmid alongside a further partial copy. Each IS66 had what has been deemed a classic organisation with the *tnpC* transposase gene accompanied by accessory proteins [34]. The presence of multiple copies of the IS66 in the genome and on the associated plasmid, with identical nucleotide sequence, is suggestive of high levels of mobility within the genome. Further transposons were identified using the Tn Central search tool [29]. In the *C. clostridioforme* LM41 chromosome, 43 transposon elements were identified from a variety of transposon element families with five of these being described as insertion sequences and one being described as an integron. These varied in size from small insertion sequences of just over 1 Kb to larger transposon elements of close to 28 Kb, and in total were predicted to comprise 497 Kb (6.3%) of the LM41 genome. Again 43 transposon elements were identified in *C. clostridioforme* LM42, while 23 were identified in each of *C. symbiosum* LM19B and LM19R. In contrast to the differences in phage presence no difference in transposon carriage, or identity, was noted between the *C. clostridioforme* LM41 and LM42 or C*. symbiosum* strains LM19B and LM19R.

Intriguingly, 23 copies, alongside two partial copies, of a gene homologous to the *ltrA* gene found in group II introns were identified in the LM41 genome. Group II introns are often termed ‘selfish’ due to their apparent lack of benefit to the host bacterium but they may alter splicing, thus increasing genetic diversity through alteration of the bacterial transcriptome [35, 36]. The *ltrA* gene encodes a protein with multiple functions that enable the excision, mobility and insertion of this intron in a genome. These functions were all predicted to be encoded in the 23 complete *ltrA* genes identified in LM41. While *ltrA* gene presence alone is insufficient to definitively confirm the presence of a functional group II intron, without identification of the surrounding RNA sequence essential to splicing, it indicates the potential presence of significant number of these introns and, to our knowledge, far more than have to date to been described in any other bacterial genome.

Secondary metabolite production in Clostridium XIVa species

To understand what potential competitive advantage may be conferred by increased genome size, antiSmash was used to determine the presence of predicted secondary metabolite encoding biosynthetic gene clusters (BGCs) in each genome [37]. *C. symbiosum* LM19B and LM19R putatively encode for a single ranthipeptide through an identified BGC, and a highly similar cluster was also found in other strains such as *C. symbiosum* WAL14163 (Table 5). In contrast *C. clostridioforme* LM41 and LM42 are predicted to encode a much larger number and variety of BGCs. In total ten BGCs were predicted in the genome of each strain and again *C. clostridioforme* YL32 was the only other sequenced *C. clostridioforme* containing a comparable number of predicted BGCs, with 13. Twenty other *C. clostridioforme* strains studied had either one or two putative BGCs, while two other strains had three and five predicted BGCs respectively. In *C. clostridioforme* LM41 and LM42 BGCs for NRPS-like (x2), transAT-PKS, lanthipeptide-class-ii, cyclic-lactone-autoinducer (x4), NRPS (butyrolactone related) and ranthipeptide were predicted. A number of these BGCs were unique with little sequence identity to known BGCs. BGCs predicted in *C. clostridioforme* YL32 were similar to those in LM41 and LM42 with the major difference being in quantity of each encoded on the YL32 genome (e.g. eight cyclic-lactone autoinducers in YL32 versus four in each of LM41 and LM42). The pCclLM41_1 and pCclLM42_1 plasmids also encoded a single BGC for an NRPS.

Discussion

Lachnospiraceae are intrinsically linked to Western disease, their presence in the human gut being associated with obesity and antibiotic use [11–13]. They possess a large number of antibiotic resistance genes that may explain their ability to respond positively to antibiotic treatment by proliferating in the months following treatment [11, 12, 38]. *Lachnospiraceae* adapt well to dysbiosis and are associated with conditions with known microbiome perturbances such as type 2 diabetes and autism spectrum disorders, as well as significantly changing in abundance over the first two years of life [20, 21, 23, 39]. Their increased presence upon dysbiosis in the human intestine has previously been linked to their often-large genome size, with their genomes being significantly larger than other commensal bacteria and potentially conferring increased metabolic flexibility [23]. However, despite their abundance in the mammalian gut microbiome and their association with specific conditions, *Lachnospiraceae* remain relatively poorly understood. Here, using recently isolated *Clostridium symbiosum* and *Clostridium clostridioforme* strains from the murine gut microbiome, we demonstrate how these strains have exceptionally large genomes even in comparison to other closely related strains. An unusual ability to acquire and maintain a significant number of MGEs seems, at least in part, to underlie this increased genome size.

Through phylogenetic relatedness and comparison to reference genomes of *Clostridia* sp. we were able to assign isolates LM19B and LM19R as *C. symbiosum* and isolates LM41 and LM42 as *C. clostridioforme*. Although the genome sizes of LM19B (5.29 Mbp) and LM19R (5.29 Mbp) were comparable to that of *C. symbiosum* reference isolate LT0011 (5 Mbp), those of isolates LM41 (7.79 Mbp) and LM42 (7.79 Mbp) are significantly larger than other sequenced *C. clostridioforme* strains with the majority of strains being between 5.5-6.5 Mb in length. LM41 and LM42 were phylogenetically most closely related to strain YL32, a strain of similarly increased genome size (7.2 Mbp), and these genomes were found to be highly similar by ANI. *C. clostridioforme* was previously reclassified into three species, *C. hathewayi*, *C. bolteae* and *C. clostridioforme* [38, 40, 41], and it has recently been suggested that these phylogenetically similar organisms should be reclassified further [42].

In conjunction with their large size *C. clostridioforme* genomes show clear evidence of genome plasticity with a smaller core genome (1898 genes) in comparison to both *C. symbiosum* (2936 genes) and *C. bolteae* (3085 genes), both of which have shorter genomes but larger core gene sets. We investigated the large accessory genome in *C. clostridioforme* strains LM41 and LM42 and determined it to be in part due to a significant increase in the presence of prophages in each genome with greater than 10% of each genome predicted to be phage derived. Present dogma dictates that evolutionary pressures would result in loss over time of such prophages with their presence negatively impacting competitiveness, due to the burden of replicating such a large collection of prophages. Therefore the presence of such a high number of prophages, particularly in direct contrast to closely related *C. clostridioforme* strains, is intriguing and certainly worthy of further study. There was scant evidence to suggest these prophages were providing any selective advantage to LM41 or LM42. No antibiotic resistance genes were found in any of the prophages and while there was a predicted increase in secondary metabolite production capability as per antiSmash analysis, none of these novel BGCs were associated with prophages [37]. Therefore the role of these prophages in the context of bacterial survival in the murine gut is unclear. During times of inflammation or perturbation of the microbiome when phages are plentiful in the gut, the possession of a large number of phages such as found in LM41 and LM42 may provide some protection against further phage infection through competitive exclusion, mediated by phages in the genome [43]. Interestingly, relatively high numbers of prophages were also predicted in *C. symbiosum* LM19B and LM19R. Whether selective pressures in the murine gut are affecting prophage infection of, and retention in, *Lachnospiracease* is worthy of further investigation as it may have ramifications for other environmental niches where such microbiome distrubances are established.

The presence of an identical and highly stable plasmid in both the LM41 and LM42 strains was interesting due to the large size of the plasmid, the difference in GC content in comparison to the genome, and an extremely large ORF carried on the plasmid. The difference in GC content indicates the plasmid likely has an origin other than related *Clostridium* XIVa strains as the GC content is substantially lower than all *Clostridium* XIVa strains sequenced to date. Also, there is no evidence that the sequenced strain most closely related phylogenetically to LM41 and LM42, YL32, carries such a plasmid. We consider that acquisition *in vivo* is the most plausible reason for its carriage and, alongside the mutliple other MGEs found in LM41 and LM42, underlines the promiscuity of these *C. clostridioforme* strains in terms of DNA acquisition.

Analysis of the LM41 genome in detail highlighted the presence of 29 identical copies of the IS66 transposase, along with 4 truncated copies and numerous other transposons. The fact that the IS66 transposase was 100% identical in each case across its total nucleotide sequence was intriguing and perhaps indicated either recent multiple acquisition events or, more likely, recent reproduction of the transposase genes and their insertion at multiple sites. The IS66 transposons were judged to be classic in that each encoded accessory ORFs such as TnpB alongside the TnpC transposase [34]. Given these findings, which indicated that LM41 was highly promiscuous in uptake of MGEs, we searched for evidence of integrative conjugative elements (ICE) and integrative and mobilizable elements (IME) as well as other MGEs such as group II introns. While ICEs and IMEs were detected, an unusually high number of copies of the group II intron-associated *ltrA* gene were detected. Although its presence is not definitive evidence of a functioning intron without identification of surrounding regions essential for splicing, we identified 23 complete *ltrA* genes. Given that the putative role of these MGEs is to alter the bacterial transcriptome through alternative splicing of bacterial genes, it is possible that the unprecedented number of *ltrA* genes found in these *C. clostridioforme* strains is indicative of further genome plasticity [35]. This alternative splicing could confer on these strains additional capabilities beyond those already afforded by the significantly increased genome size.

Given the increased gene flow seen as a result of HGT in *C. clostridioforme* strains LM41, LM42 and YL32 it raises the question of whether defence systems to combat phage and MGEs are present in lower numbers or are less efficient in these strains. While a lack of such systems, be they restriction modification, CRISPR-Cas or similar, would expose the strains to increased risk due to increased virulent phage infection or propagation, it would explain the increased presence of phage and MGEs in these strains, their widespread distribution in the genomes and the significantly increased size comparable to other *C. clostridioforme* genomes.

In conclusion, we have characterised the genome sequences of newly isolated and highly unusual strains of *Lachnospiraceae*. Our study has revealed that while the *C. symbiosum* strains identified have similar genome sequences to those of the reference strains, the genomes of the newly sequenced *C. clostridioforme* strains are substantially larger than those previously sequenced, with the single exception of *C. clostridioforme* YL32. YL32's genome is not as large as the two *C. clostridioforme* strains identified here but shows similar increases in secondary metabolite production capability and prophage presence. Additionally, *C. clostridioforme* YL32 and the strains isolated here form a monophyletic clade with unusually long branch length in the *C. clostridioforme* phylogenetic tree, consistent with the proposition that increased MGE presence may be a significant evolutionary driver. This work highlights both the potential capabilities and extraordinary complexity within the gut microbiome and emphasizes the significant gaps in our known as regards specific species, the role of MGEs in shaping species evolution in the intestine and the untapped secondary metabolite capabilities of many yet to be identified strains.

References

1. Nemet I, Saha PP, Gupta N, Zhu W, Romano KA, Skye SM, et al. A Cardiovascular Disease-Linked Gut Microbial Metabolite Acts via Adrenergic Receptors. Cell. 2020;180:862-877.e22.

2. Quinn RA, Melnik A V., Vrbanac A, Fu T, Patras KA, Christy MP, et al. Global chemical effects of the microbiome include new bile-acid conjugations. Nature. 2020;579:1–19. doi:10.1038/s41586-020-2047-9.

3. Foster JA, McVey Neufeld KA. Gut-brain axis: How the microbiome influences anxiety and depression. Trends in Neurosciences. 2013.

4. Carding S, Verbeke K, Vipond DT, Corfe BM, Owen LJ. Dysbiosis of the gut microbiota in disease. Microb Ecol Heal Dis. 2015.

5. Dalile B, Van Oudenhove L, Vervliet B, Verbeke K. The role of short-chain fatty acids in microbiota–gut–brain communication. Nature Reviews Gastroenterology and Hepatology. 2019.

6. Fröhlich EE, Farzi A, Mayerhofer R, Reichmann F, Jačan A, Wagner B, et al. Cognitive Impairment by Antibiotic-Induced Gut Dysbiosis: Analysis of Gut Microbiota-Brain Communication. Brain Behav Immun. 2016.

7. Yano JM, Yu K, Donaldson GP, Shastri GG, Ann P, Ma L, et al. Indigenous bacteria from the gut microbiota regulate host serotonin biosynthesis. Cell. 2015;161:264–76. doi:10.1016/j.cell.2015.02.047.

8. Patterson E, Ryan PM, Wiley N, Carafa I, Sherwin E, Moloney G, et al. Gamma-aminobutyric acid-producing lactobacilli positively affect metabolism and depressive-like behaviour in a mouse model of metabolic syndrome. Sci Rep. 2019;9:16323. doi:10.1038/s41598-019-51781-x.

9. Hulme H, Meikle LM, Strittmatter N, van der Hooft JJJ, Swales J, Bragg RA, et al. Microbiome-derived carnitine mimics as previously unknown mediators of gut-brain axis communication. Sci Adv. 2020;6:eaax6328.

10. Hulme H, Meikle LM, Strittmatter N, Swales J, Hamm G, Brown SL, et al. Mapping the

Influence of the Gut Microbiota on Small Molecules across the Microbiome Gut Brain Axis. J Am Soc Mass Spectrom. 2022;33:649–59. doi:10.1021/JASMS.1C00298.

11. Raymond F, Ouameur AA, Déraspe M, Iqbal N, Gingras H, Dridi B, et al. The initial state of the human gut microbiome determines its reshaping by antibiotics. ISME J. 2016;10:707–20.

12. Palleja A, Mikkelsen KH, Forslund SK, Kashani A, Allin KH, Nielsen T, et al. Recovery of gut microbiota of healthy adults following antibiotic exposure. Nat Microbiol. 2018;3:1255–65. doi:10.1038/s41564-018-0257-9.

13. Le Chatelier E, Nielsen T, Qin J, Prifti E, Hildebrand F, Falony G, et al. Richness of human gut microbiome correlates with metabolic markers. Nature. 2013;500:541–6. doi:10.1038/nature12506.

14. Pryde SE, Duncan SH, Hold GL, Stewart CS, Flint HJ. The microbiology of butyrate formation in the human colon. FEMS Microbiol Lett. 2002;217:133–9. doi:10.1111/j.1574-6968.2002.tb11467.x.

15. Jafari N V., Kuehne SA, Bryant CE, Elawad M, Wren BW, Minton NP, et al. Clostridium difficile Modulates Host Innate Immunity via Toxin-Independent and Dependent Mechanism(s). PLoS One. 2013;8:e69846. doi:10.1371/JOURNAL.PONE.0069846.

16. Chen H, Ma X, Liu Y, Ma L, Chen Z, Lin X, et al. Gut Microbiota Interventions With Clostridium butyricum and Norfloxacin Modulate Immune Response in Experimental Autoimmune Encephalomyelitis Mice. Front Immunol. 2019;10:1662.

17. Wells CL, Wilkins TD. Clostridia: Sporeforming Anaerobic Bacilli. Med Microbiol. 1996. https://www.ncbi.nlm.nih.gov/books/NBK8219/. Accessed 4 May 2022.

18. Lozupone C, Faust K, Raes J, Faith JJ, Frank DN, Zaneveld J, et al. Identifying genomic and metabolic features that can underlie early successional and opportunistic lifestyles of human gut symbionts. Genome Res. 2012;22:1974–84. doi:10.1101/gr.138198.112.

19. Karlsson FH, Tremaroli V, Nookaew I, Bergström G, Behre CJ, Fagerberg B, et al. Gut metagenome in European women with normal, impaired and diabetic glucose control. 2013. doi:10.1038/nature12198.

20. Qin J, Li Y, Cai Z, Li S, Zhu J, Zhang F, et al. A metagenome-wide association study of gut microbiota in type 2 diabetes. Nature. 2012;490:55–60. doi:10.1038/nature11450.

21. Finegold SM, Molitoris D, Song Y, Liu C, Vaisanen M, Bolte E, et al. Gastrointestinal Microflora Studies in Late-Onset Autism. Clin Infect Dis. 2002.

22. Xie YH, Gao QY, Cai GX, Sun XM, Zou TH, Chen HM, et al. Fecal Clostridium symbiosum for Noninvasive Detection of Early and Advanced Colorectal Cancer: Test and Validation Studies. EBioMedicine. 2017;25:32–40.

23. Lozupone C, Faust K, Raes J, Faith JJ, Frank DN, Zaneveld J, et al. Identifying genomic and metabolic features that can underlie early successional and opportunistic lifestyles of human gut symbionts. Genome Res. 2012.

24. Yatsunenko T, Rey FE, Manary MJ, Trehan I, Dominguez-Bello MG, Contreras M, et al. Human gut microbiome viewed across age and geography. Nature. 2012;486:222–7.

25. Stanislawski MA, Dabelea D, Wagner BD, Iszatt N, Dahl C, Sontag MK, et al. Gut Microbiota in the First 2 Years of Life and the Association with Body Mass Index at Age 12 in a Norwegian Birth Cohort. MBio. 2018;9. doi:10.1128/mBio.01751-18.

26. Thomson SR, Seo SS, Barnes SA, Louros SR, Muscas M, Dando O, et al. Cell-Type-Specific Translation Profiling Reveals a Novel Strategy for Treating Fragile X Syndrome. Neuron. 2017;95:550-563.e5. doi:10.1016/j.neuron.2017.07.013.

27. Pritchard L, Glover RH, Humphris S, Elphinstone JG, Toth IK. Genomics and taxonomy in diagnostics for food security: Soft-rotting enterobacterial plant pathogens. Analytical Methods. 2016;8:12–24. doi:10.1039/c5ay02550h.

28. Ross K, Varani AM, Snesrud E, Huang H, Alvarenga DO, Zhang J, et al. TnCentral: a Prokaryotic Transposable Element Database and Web Portal for Transposon Analysis. MBio. 2021;12. doi:10.1128/MBIO.02060-21.

29. Liu M, Li X, Xie Y, Bi D, Sun J, Li J, et al. ICEberg 2.0: an updated database of bacterial integrative and conjugative elements. Nucleic Acids Res. 2019;47:D660–5. doi:10.1093/NAR/GKY1123.

30. Aziz RK, Bartels D, Best A, DeJongh M, Disz T, Edwards RA, et al. The RAST Server:

rapid annotations using subsystems technology. BMC Genomics. 2008;9. doi:10.1186/1471-2164-9-75.

31. Altschul SF, Gish W, Miller W, Myers EW, Lipman DJ. Basic local alignment search tool. J Mol Biol. 1990.

32. Arndt D, Grant JR, Marcu A, Sajed T, Pon A, Liang Y, et al. PHASTER: a better, faster version of the PHAST phage search tool. Nucleic Acids Res. 2016;44:W16–21. doi:10.1093/nar/gkw387.

33. Hae JK, Paterson NG, Gaspar AH, Hung TT, Baker EN. The Corynebacterium diphtheriae shaft pilin SpaA is built of tandem Ig-like modules with stabilizing isopeptide and disulfide bonds. Proc Natl Acad Sci U S A. 2009;106:16967–71. doi:10.1073/PNAS.0906826106/SUPPL_FILE/0906826106SI.PDF.

34. Gourbeyre E, Siguier P, Chandler M. Route 66: investigations into the organisation and distribution of the IS66 family of prokaryotic insertion sequences. Res Microbiol. 2010;161:136–43. doi:10.1016/J.RESMIC.2009.11.005.

35. LaRoche-Johnston F, Monat C, Coulombe S, Cousineau B. Bacterial group II introns generate genetic diversity by circularization and trans-splicing from a population of intron-invaded mRNAs. PLoS Genet. 2018;14. doi:10.1371/JOURNAL.PGEN.1007792.

36. Toro N, Martínez-Abarca F, Molina-Sánchez MD, García-Rodríguez FM, Nisa-Martínez R. Contribution of Mobile Group II Introns to Sinorhizobium meliloti Genome Evolution. Front Microbiol. 2018;9 APR. doi:10.3389/FMICB.2018.00627.

37. Blin K, Shaw S, Kloosterman AM, Charlop-Powers Z, Van Wezel GP, Medema MH, et al. AntiSMASH 6.0: Improving cluster detection and comparison capabilities. Nucleic Acids Res. 2021;49:W29–35. doi:10.1093/nar/gkab335.

38. Dehoux P, Marvaud JC, Abouelleil A, Earl AM, Lambert T, Dauga C. Comparative genomics of Clostridium bolteae and Clostridium clostridioforme reveals species-specific genomic properties and numerous putative antibiotic resistance determinants. BMC Genomics. 2016.

39. Karlsson FH, Tremaroli V, Nookaew I, Bergström G, Behre CJ, Fagerberg B, et al. Gut

metagenome in European women - supply. Nature. 2013;498:99–103. doi:10.1038/nature12198.

40. Finegold SM, Song Y, Liu C, Hecht DW, Summanen P, Könönen E, et al. Clostridium clostridioforme: A mixture of three clinically important species. Eur J Clin Microbiol Infect Dis. 2005;24:319–24. doi:10.1007/s10096-005-1334-6.

41. Haas KN, Blanchard JL. Reclassification of the clostridium clostridioforme and clostridium sphenoides clades as enterocloster gen. Nov. and lacrimispora gen. nov., including reclassification of 15 taxa. Int J Syst Evol Microbiol. 2020.

42. Schaubeck M, Clavel T, Calasan J, Lagkouvardos I, Haange SB, Jehmlich N, et al. Dysbiotic gut microbiota causes transmissible Crohn’s disease-like ileitis independent of failure in antimicrobial defence. Gut. 2016.

43. Rocha EPC, Bikard D. Microbial defenses against mobile genetic elements and viruses: Who defends whom from what? PLOS Biol. 2022;20:e3001514. doi:10.1371/JOURNAL.PBIO.3001514.

Figures

Figure 1

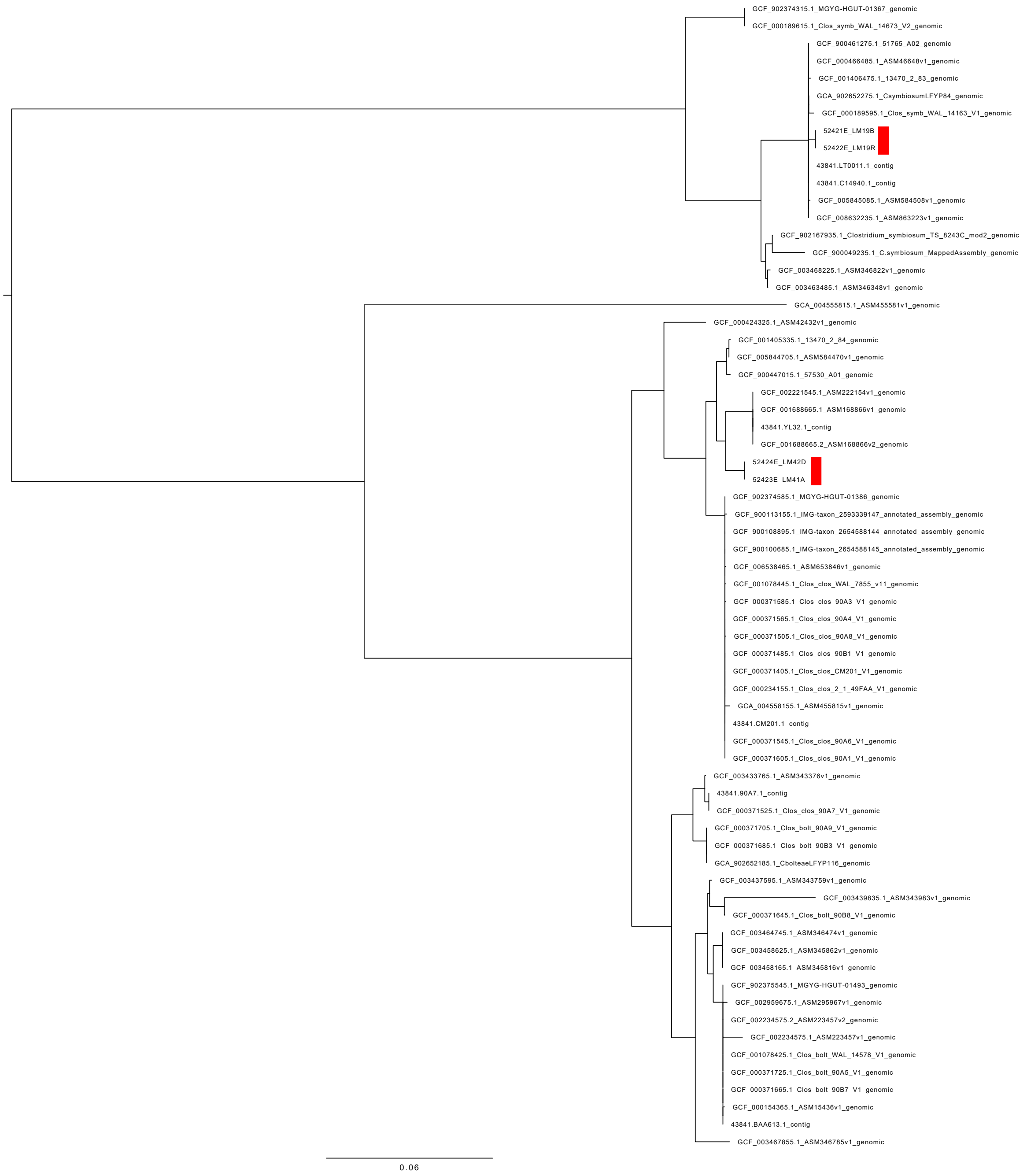
GCF_902374315.1_MGYG-HGUT-01367_genomic
GCF_000189615.1_Clos_symb_WAL_14673_V2_genomic
GCF_900461275.1_51765_A02_genomic
GCF_000466485.1_ASM46648v1_genomic
GCF_001406475.1_13470_2_83_genomic
GCA_902652275.1_CsymbiosumLFYP84_genomic
GCF_000189595.1_Clos_symb_WAL_14163_V1_genomic
52421E_LM19B
52422E_LM19R
43841.LT0011.1_contig
43841.C14940.1_contig
GCF_005845085.1_ASM584508v1_genomic
GCF_008632235.1_ASM863223v1_genomic
GCF_902167935.1_Clostridium_symbiosum_TS_8243C_mod2_genomic
GCF_900049235.1_C.symbiosum_MappedAssembly_genomic
GCF_003468225.1_ASM346822v1_genomic
GCF_003463485.1_ASM346348v1_genomic
GCA_004555815.1_ASM455581v1_genomic
GCF_000424325.1_ASM42432v1_genomic
GCF_001405335.1_13470_2_84_genomic
GCF_005844705.1_ASM584470v1_genomic
GCF_900447015.1_57530_A01_genomic
GCF_002221545.1_ASM222154v1_genomic
GCF_001688665.1_ASM168866v1_genomic
43841.YL32.1_contig
GCF_001688665.2_ASM168866v2_genomic
52424E_LM42D
52423E_LM41A
GCF_902374585.1_MGYG-HGUT-01386_genomic
GCF_900113155.1_IMG-taxon_2593339147_annotated_assembly_genomic
GCF_900108895.1_IMG-taxon_2654588144_annotated_assembly_genomic
GCF_900100685.1_IMG-taxon_2654588145_annotated_assembly_genomic
GCF_006538465.1_ASM653846v1_genomic
GCF_001078445.1_Clos_clos_WAL_7855_v11_genomic
GCF_000371585.1_Clos_clos_90A3_V1_genomic
GCF_000371565.1_Clos_clos_90A4_V1_genomic
GCF_000371505.1_Clos_clos_90A8_V1_genomic
GCF_000371485.1_Clos_clos_90B1_V1_genomic
GCF_000371405.1_Clos_clos_CM201_V1_genomic
GCF_000234155.1_Clos_clos_2_1_49FAA_V1_genomic
GCA_004558155.1_ASM455815v1_genomic
43841.CM201.1_contig
GCF_000371545.1_Clos_clos_90A6_V1_genomic
GCF_000371605.1_Clos_clos_90A1_V1_genomic
GCF_003433765.1_ASM343376v1_genomic
43841.90A7.1_contig
GCF_000371525.1_Clos_clos_90A7_V1_genomic
GCF_000371705.1_Clos_bolt_90A9_V1_genomic
GCF_000371685.1_Clos_bolt_90B3_V1_genomic
GCA_902652185.1_CbolteaeLFYP116_genomic
GCF_003437595.1_ASM343759v1_genomic
GCF_003439835.1_ASM343983v1_genomic
GCF_000371645.1_Clos_bolt_90B8_V1_genomic
GCF_003464745.1_ASM346474v1_genomic
GCF_003458625.1_ASM345862v1_genomic
GCF_003458165.1_ASM345816v1_genomic
GCF_902375545.1_MGYG-HGUT-01493_genomic
GCF_002959675.1_ASM295967v1_genomic
GCF_002234575.2_ASM223457v2_genomic
GCF_002234575.1_ASM223457v1_genomic
GCF_001078425.1_Clos_bolt_WAL_14578_V1_genomic
GCF_000371725.1_Clos_bolt_90A5_V1_genomic
GCF_000371665.1_Clos_bolt_90B7_V1_genomic
GCF_000154365.1_ASM15436v1_genomic
43841.BAA613.1_contig
GCF_003467855.1_ASM346785v1_genomic
0.06

Figure 1: Identification of phylogenetic lineages of *Clostridia* isolates. Phylogenetic rooted gene tree of *Clostridium* XIVa cluster created with single copy orthologs (OrthoFinder v2.5.2). New strains identified, LM19B, LM19R, LM41 and LM42 are highlighted with red and can be seen to fall into previously identified *C. symbiosum* and *C. clostridioforme* respectively.

Figure 2

a

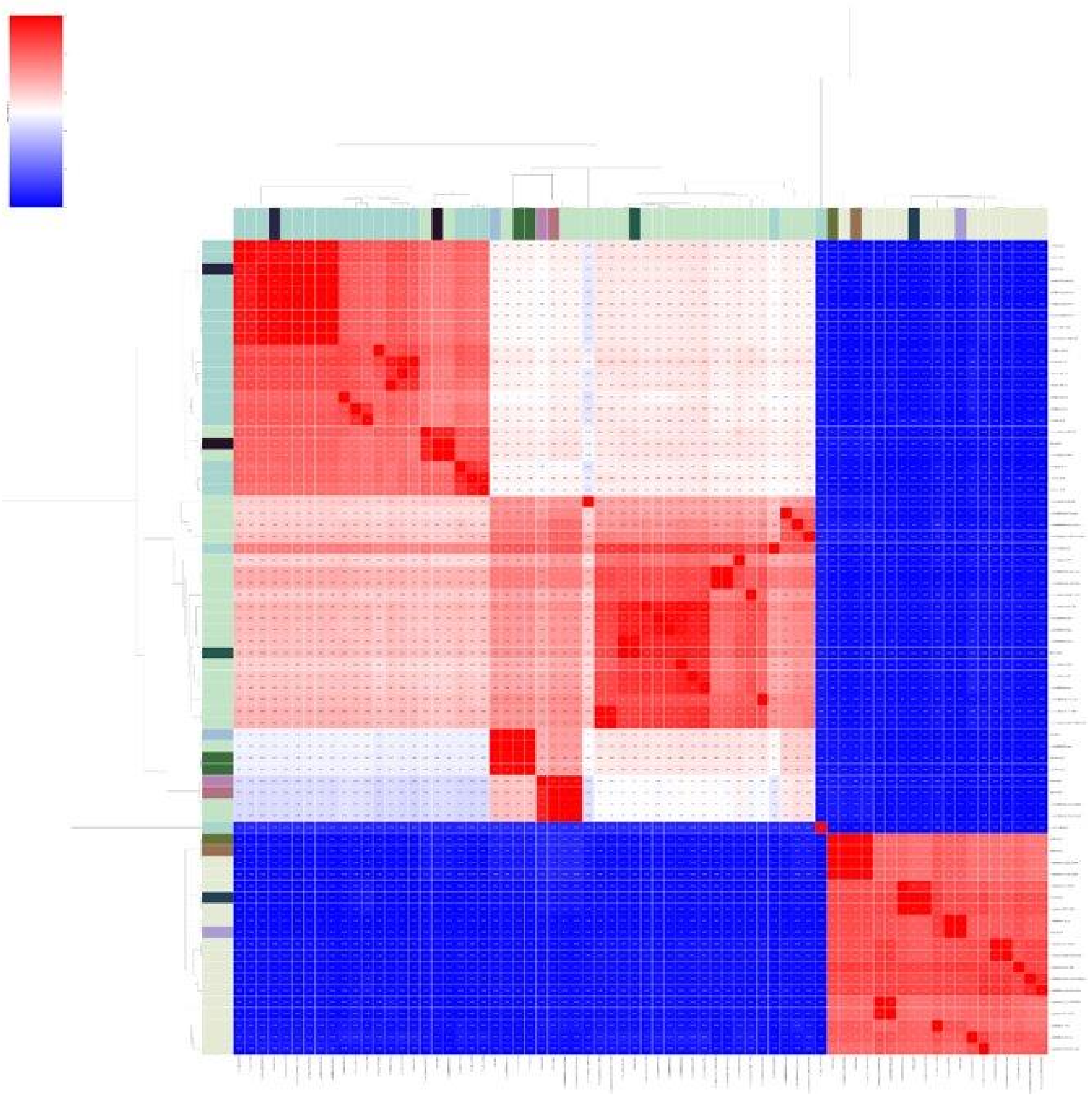

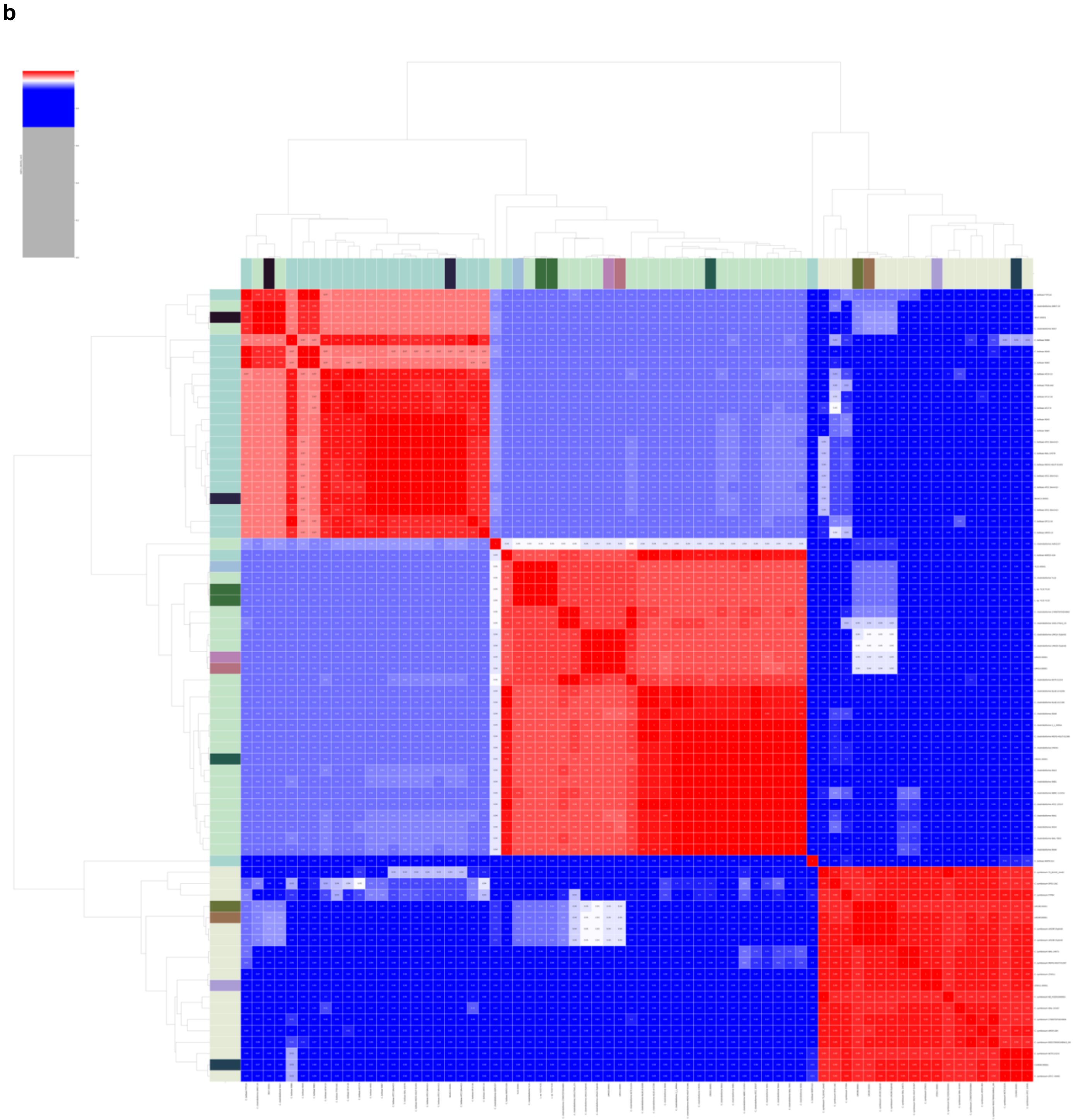

Figure 2: ANIm (Average Nucleotide Identity using MUMmer) comparisons of *Clostridium* XIVa cluster genomes obtained using pyani v0.3+. (**a**) shows a heat map of genome percent coverage: pairwise comparisons where the alignable fraction of genome is greater than 50% are indicated in red; blue cells indicate that the alignable fraction is less than 50% of the genome. *C. bolteae* and *C. clostridioforme* are generally alignable over 50% of their genome sequence but share less than 5% of alignable genome sequence with *C.*

symbiosum. This indicates that *C. bolteae*/*C. clostridioforme* are likely to correspond to the same genus, but that they are genomically quite distinct from *C. symbiosum*. (**b**) is a heat map of ANIm percentage identity, where red cells indicate an identity greater than 95% (an approximate threshold for bacterial species boundaries), and blue cells an identity less than 95%. The heat map confirms that the sequenced *C. bolteae*, *C. symbiosum*, and *C. clostridioforme* isolates support division into the three species groups, but that isolate W0P9.022 may be a member of a distinct species; this conclusion is also supported by the genome coverage data, which suggests that W0P9.022 may also be the sole representative of a distinct genus.

Figure 3

(a) *C. clostridioforme*

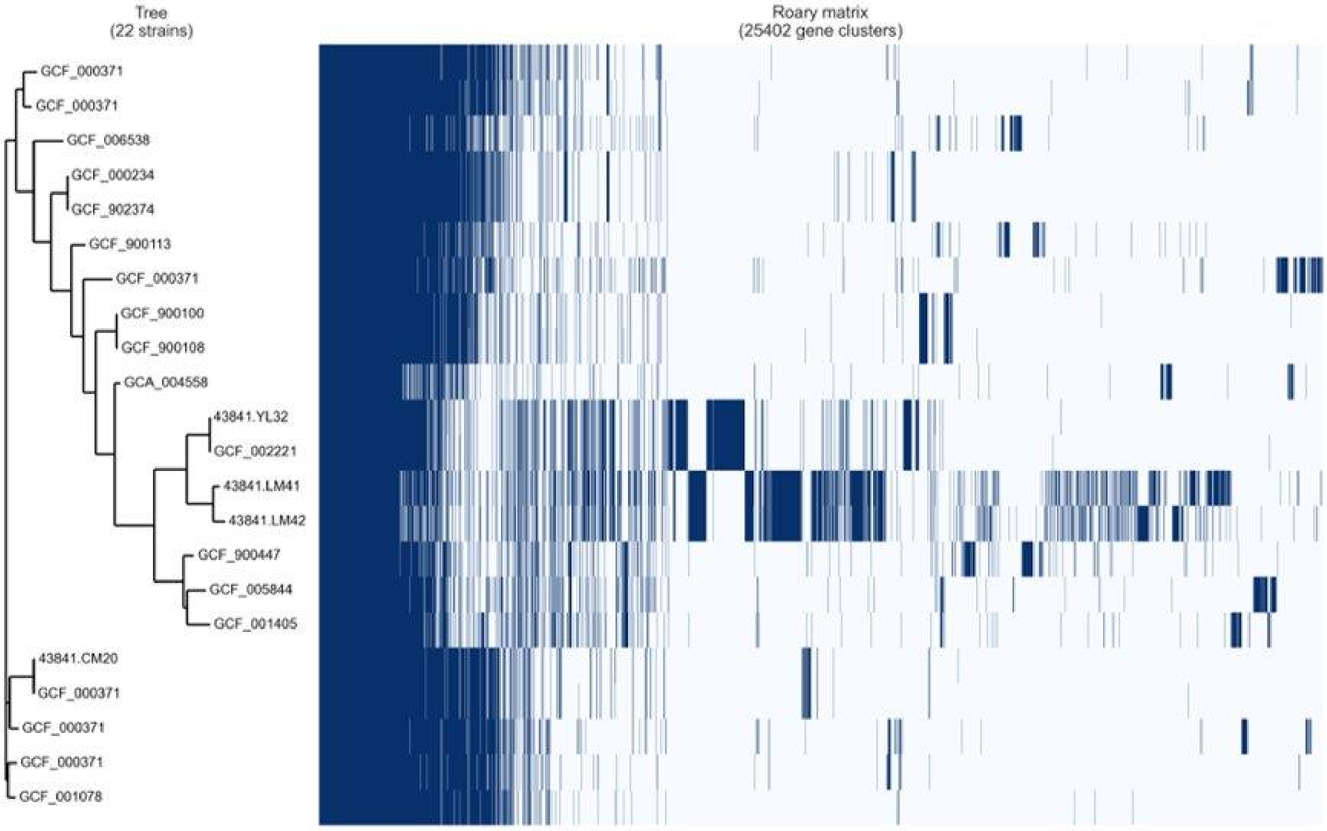

(b) *C. symbiosum*

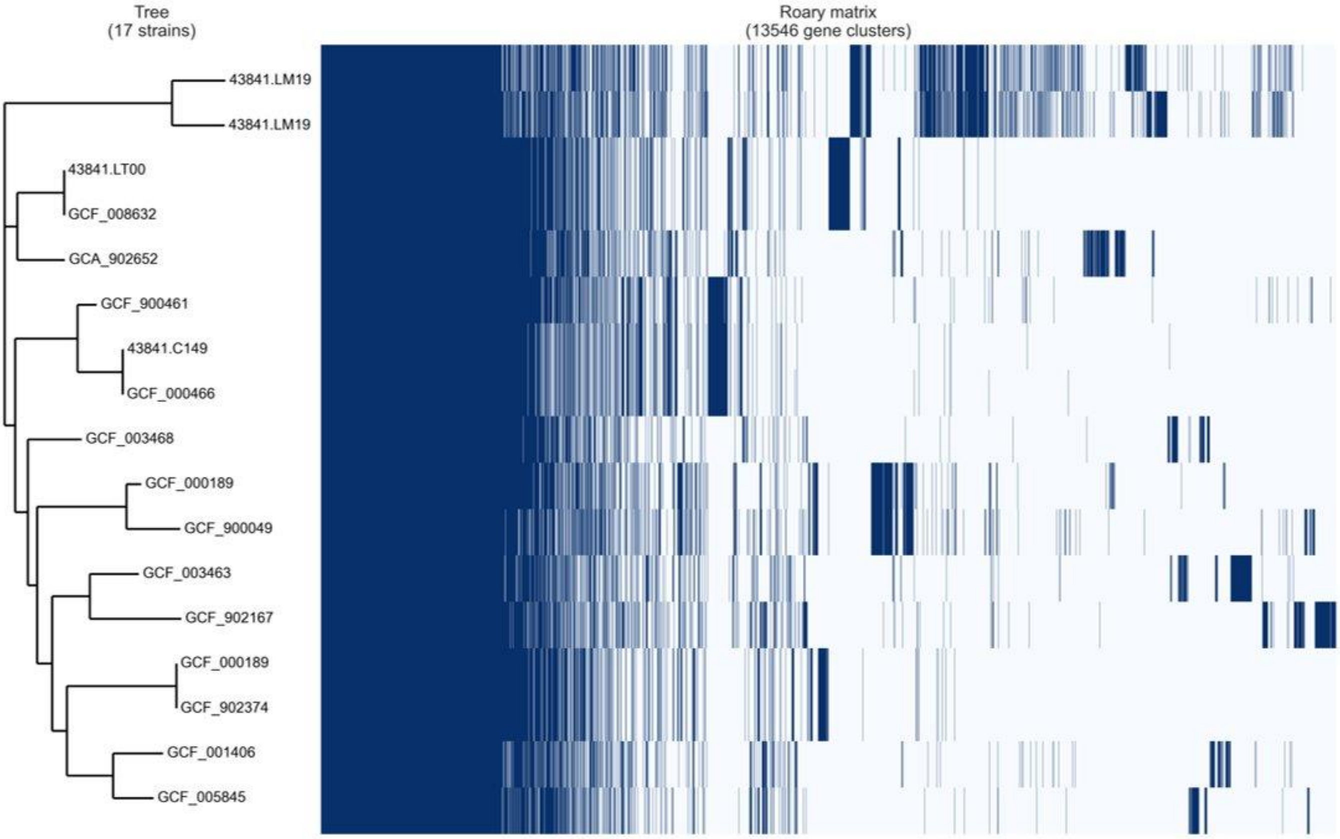

(c) *C. bolteae*

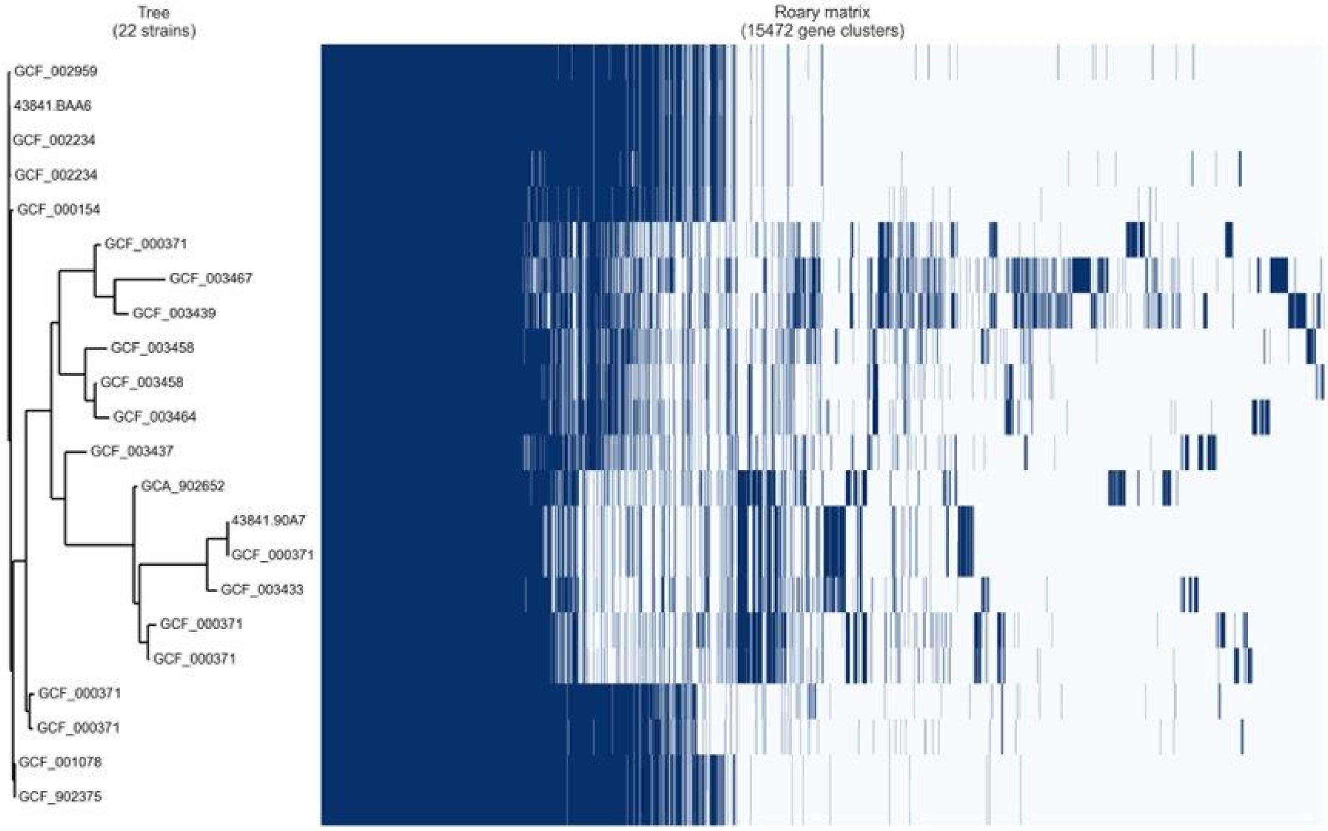

Figure 3: **Roary analysis of gene presence/absence in *Clostridium* XIVa species.** Roary analysis of the presence/absence of genes across; (a) 22 strains of *C. clostridioforme*, (b) 17 strains of *C. symbiosum* and, (c) 22 strains of *C. bolteae*. New isolates LM41, LM42 and LM19B, LM19R are shown in the *C. clostridioforme* and *C. symbiosum* analysis respectively.

Table 1

Strain	**Genome size (Kbp)**	**GC skew (%)**
C. clostridioforme LM42	7975223	47.84
C. clostridioforme LM41	7977041	47.85
C. clostridioforme YL32	7157460	48.11
C. clostridioforme CM201	5586179	49.16
C. clostridioforme NBRC11352	5687315	48.92
C. clostridioforme 90A8	5974284	48.5
C clostridioforme 90A1	5806027	48.42
C. clostridioforme CM201	5655915	48.55
C. clostridioforme 90A7	6033914	48.23
C. clostridioforme LT001.00001	5072209	47.89
C. clostridioforme AGR2157	4943165	49.01
C. clostridioforme NCTC11224	5827564	48.97
C. clostridioforme 90A7	6158650	49.22
C._clostridioforme 90A4	5871489	48.15
C. clostridioforme AM07-19	6231573	49.25
C. clostridioforme 1001175	5676948	48.96
C. clostridioforme 90B1	5602152	48.48
C. clostridioforme NLAE-zl-C196	5225716	49.1
C. clostridioforme 2_1_49FAA	5500475	48.53
C. clostridioforme 2789STDY5834865	5514222	49.14
C clostridioforme 90A3	5549890	48.37
C. bolteae AM35-14	6793441	48.62
C. bolteae LFYP116	6597056	49.18
C. bolteae 90B8	6482686	48.37
C. bolteae 90B3	6538460	48.94
C. bolteae 90A9	6377378	49.48
C. bolteae OF13-16	6539152	48.65
C. bolteae AF24-13	6422063	48.95
C. bolteae 90B7	6439235	48.78

C. bolteae MGYG-HGUT-01493	6604884	48.89
C. bolteae ATCC BAA-613	6557988	49.05
C. bolteae BAA613.00001	6570176	49.1
C. bolteae TF09-4AC	6232356	49.35
C. bolteae 90A5	6421395	48.87
C. bolteae AF14-18	6430942	49.07
C. bolteae W0P25.026	4404879	50.86
C bolteae AF27-9	6144412	49.17
C. symbiosum WAL-14163	5352498	47.36
C. symbiosum LM19R	5298804	47.68
C. symbiosum LM19B	5299950	47.68
C. symbiosum NCTC13233	5054777	47.8
C. symbiosum MGYG-HGUT-001367	4916964	47.59
C. symbiosum ATCC 14940	4823675	47.51
C. symbiosum FYP84	5351947	47.9
C symbiosum 2789STDY5834864	4727130	47.91
C. symbiosum OF01-1AC	5075475	47.79
C. symbiosum BSD278006168	4763759	47.85
C. symbiosum TS8243C	5266075	47.92
C. symbiosum AM39-1BH	4767382	47.97

Table 1: Genome size and GC percentage of *Clostridium* XIVa strains. Genome size and GC skew of isolated strains *C. clostridioforme* LM41 and LM42, and *C. symbiosum* LM19B and LM19R, in comparison with selected published *C. clostridioforme*, *C. symbiosum* and *C. bolteae* genomes.

Table 2

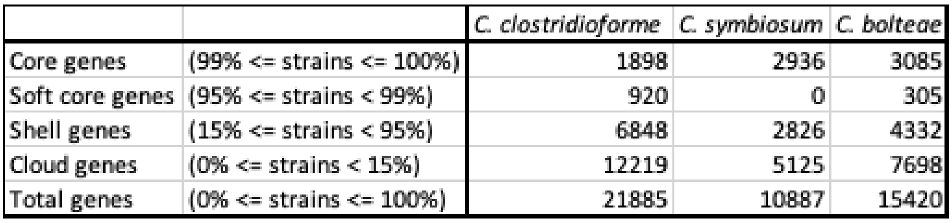

		C. clostridioforme	*C. symbiosum*	*C. bolteae*
Core genes	(99% <= strains <= 100%)	1898	2936	3085
Soft core genes	(95% <= strains < 99%)	920	0	305
Shell genes	(15% <= strains < 95%)	6848	2826	4332
Cloud genes	(0% <= strains < 15%)	12219	5125	7698
Total genes	(0% <= strains <= 100%)	21885	10887	15420

Table 2: Pangenome analysis using Roary of *Clostridium* XIVa species. Pangenome analysis using Roary of the 55 genomes of *C. clostridioforme*, *C. bolteae* and *C. symbiosum* (excluding W0P9.022) from Figure 2 which had first been annotated using Prokka. Core, soft core, shell, cloud and total genes for each strain are indicated.

Table 3:

Clostridium clostridioforme

Strain	Number of Phage	Genome size (bp)	Phage bp (kbp)	%Genome = phage
C. clostridioforme LM42	28	7975223	894	12.6249378
C. clostridioforme LM41	29	7977041	878.2	12.3710335
C. clostridioforme YL32	21	7157460	566.8	8.60004916
C. clostridioforme CM201	12	5586179	293.2	5.53941363
C. clostridioforme NBRC11352	14	5687315	294.7	5.46488114
C. clostridioforme 90A8	17	5974284	307.3	5.42263751
C clostridioforme 90A1	14	5806027	272.5	4.92452644
C. clostridioforme CM201	12	5655915	243.3	4.49505461
C. clostridioforme 90A7	13	6033914	248.7	4.29889024
C. clostridioforme LT001.00001	2	5072209	208.4	4.28470773
C. clostridioforme AGR2157	10	4943165	199.7	4.2100026
C. clostridioforme NCTC11224	11	5827564	228.3	4.07732159
C. clostridioforme 90A7	11	6158650	224.6	3.78493609
C. clostridioforme 90A4	13	5871489	208.1	3.6744783
C. clostridioforme AM07-19	9	6231573	186.3	3.08174668
C. clostridioforme 1001175	6	5676948	167.9	3.04771351
C. clostridioforme 90B1	12	5602152	163.5	3.00625964
C. clostridioforme NLAE-zl-C196	8	5225716	150.9	2.97350682
C. clostridioforme 2_1_49FAA	8	5500475	129.3	2.40729449
C. clostridioforme 2789STDY5834865	8	5514222	124.2	2.30425776
C. clostridioforme 90A3	8	5549890	107.7	1.97898273

Clostridium symbiosum

Strain	Number of Phage	Genome size (bp)	Phage bp (kbp)	%Genome = phage
C. symbiosum WAL-14163	12	5352498	352.4	7.04786186
C. symbiosum LM19R	8	5298804	250.6	4.9641417

C. symbiosum LM19B	8	5299950	250.2	4.95470073
C. symbiosum NCTC13233	0	5054777	153	3.12131702
C. symbiosum MGYG-HGUT-001367	4	4916964	126.8	2.647091
C. symbiosum WAL-14673	4	4916964	126.8	2.647091
C. symbiosum ATCC 14940	4	4823675	106.8	2.26421094
C. symbiosum FYP84	4	5351947	114.8	2.19203318
C. symbiosum 2789STDY5834864	2	4727130	65.6	1.40726328
C. symbiosum OF01-1AC	4	5075475	70.4	1.40657233
C. symbiosum BSD278006168	3	4763759	40.9	0.86600087
C. symbiosum TS8243C	2	5266075	21.3	0.40611847
C. symbiosum AM39-1BH	1	4767382	7.3	0.1533587

Clostridium bolteae

Strain	**Number of Phage**	**Genome size (bp)**	**Phage bp (kbp)**	**%Genome = phage**
C. bolteae AM35-14	22	6793441	460.1	7.26472805
C. bolteae LFYP116	6	6597056	290.3	4.60300034
C. bolteae 90B8	12	6482686	247.9	3.97607873
C. bolteae 90B3	13	6538460	243.4	3.86652391
C. bolteae 90A9	10	6377378	219.1	3.55781275
C. bolteae OF13-16	11	6539152	223.9	3.54538505
C. bolteae AF24-13	8	6422063	194.5	3.12321208
C. bolteae 90B7	8	6439235	185.9	2.97281371
C. bolteae WAL-14578	7	6604884	180.7	2.8128086
C. bolteae ATCC BAA-613	7	6557988	175.8	2.75454123
C. bolteae BAA613.00001	7	6570176	172	2.68826616
C. bolteae TF09-4AC	5	6232356	143	2.34835999
C. bolteae 90A5	6	6421395	145.9	2.3249162
C. bolteae AF14-18	6	6430942	113.7	1.79983607
C. bolteae W0P25.026	1	4404879	20.4	0.46527763
C. bolteae AF27-9	1	6144412	10.4	0.16954646

Table 3: Putative phage content of *Clostridium* XIVa species. Analysis of the putative phage content of the genomes of listed *Clostridium* XIVa species using Phaster. The number of phage, total genome size, putative phage material detected, and the percentage of the total genome occupied by this phage material is indicated.

Table 4: IMEs and ICEs

Clostridium symbiosum LM19B

Name	Location	Length/bp	Type
Region1	177767..254712	76946	Putative ICE with T4SS
Region2	2298904..2328641	29738	Putative IME
Region3	4467243..4543305	76063	Putative ICE with T4SS

Clostridium symbiosum LM19R

Name	Location	Length/bp	Type
Region1	890897..977449	86553	Putative ICE with T4SS
Region2	1881404..1911154	29751	Putative IME
Region3	2874565..2965979	91415	Putative ICE with T4SS
Region4	3082855..3135714	52860	Putative ICE with T4SS
Region5	4627784..4655274	27491	Putative IME
Region6	5230762..5235310	4549	Putative IME without identified DR

Clostridium clostridioforme LM41

Name	Location	Length/bp	Type
Region1	531191..724491	193301	Putative ICE with T4SS
Region2	1197371..1199761	2391	Putative IME without identified DR
Region3	2041831..2195442	153612	Putative ICE with T4SS
Region4	2336403..2354509	18107	Putative IME without identified DR
Region5	2623858..2640032	16175	Putative IME
Region6	3029722..3033702	3981	Putative IME without identified DR
Region7	3193104..3340431	147328	Putative ICE with T4SS
Region8	3731406..3818133	86728	Putative ICE with T4SS
Region9	4910211..4945863	35653	Putative ICE with T4SS
Region10	5423367..5478842	55476	Putative AICE with Rep and Tra
Region11	5947737..6062237	114501	Putative ICE with T4SS
Region12	7206164..7398777	192614	Putative ICE with T4SS
Region13	7835678..7848309	12632	Putative IME

Clostridium clostridioforme LM42

Name	Location	Length/bp	Type
Region1	530235..641955	111721	Putative ICE with T4SS
Region2	1089702..1133607	43906	Putative IME without identified DR
Region3	1695836..1717892	22057	Putative IME without identified DR
Region4	1945247..2001257	56011	Putative ICE with T4SS
Region5	2441505..2448548	7044	Putative IME without identified DR
Region6	2586949..2658045	71097	Putative ICE with T4SS
Region7	2892979..2914638	21660	Putative ICE with T4SS
Region8	3167058..3186257	19200	Putative IME without identified DR
Region9	3512594..3525203	12610	Putative IME

Region10	3891579..3924258	32680	Putative IME
Region11	4552655..4651363	98709	Putative ICE with T4SS
Region12	4874134..4938049	63916	Putative ICE with T4SS
Region13	5264895..5487459	222565	Putative ICE with T4SS
Region14	5648469..5652450	3982	Putative IME without identified DR
Region15	6051571..6091699	40129	Putative IME
Region16	6398610..6425203	26594	Putative IME
Region17	7221062..7303454	82393	Putative ICE with T4SS

Table 4: Putative integrative conjugative elements (ICEs) and integrative mobile elements (IMEs) detected in *Clostridium symbiosum* LM19B and LM19 R and *Clostridium clostridioforme* strains LM41 and LM42. Identification of putative ICEs and IMEs in each strain was carried out using ICEfinder (Add ref). ICEs were detected with and without type 4 secretion systems (T4SS) while IMEs were examined for presence of direct repeats (DR).

Table 5: antiSmash analysis of *Clostridium XIVa* genomes

C. clostridioforme

Strain	BGCs	Putative metabolite(s)
YL32	13	cyclic-lactone-autoinducer (x8), ranthipeptide, transAT-PKS, NRPS, Tyrosine recombinase XerC, ranthipeptide, NRPS
LM41	10	NRPS-like (x2), transAT-PKS, lanthipeptide-class-ii, cyclic-lactone-autoinducer (x4), NRPS (butyrolactone related), ranthipeptide
LM42	10	NRPS-like (x2), transAT-PKS, lanthipeptide-class-ii, cyclic-lactone-autoinducer (x4), NRPS (butyrolactone related), ranthipeptide
GCF_900113155.1_IMG-taxon_2593339147	5	ranthipeptide, cyclic-lactone-autoinduce, NRPS-like (x3)
GCF_005844705.1_ASM584470v1	4	ranthipeptide, NRPS-like, cyclic-lactone-autoinducer, butyrolactone
GCF_006538465.1_ASM653846v1_	3	cyclic-lactone-autoinducer, ranthipeptide, NRPS
GCF_000371505.1_Clos_clos_90A8_V1	3	cyclic-lactone-autoinducer, ranthipeptide, RRE-containing
43841.BAA613.1_	2	NRPS-like, ranthipeptide
43841.CM201.1	2	cyclic-lactone-autoinducer, ranthipeptide
GCF_000234155.1_Clos_clos_2_1_49FAA_V1	2	cyclic-lactone-autoinducer, ranthipeptide
GCF_000371545.1_Clos_clos_90A6_V	2	cyclic-lactone-autoinducer, ranthipeptide
GCF_000371565.1_Clos_clos_90A4_V1	2	cyclic-lactone-autoinducer, ranthipeptide
GCF_000371585.1_Clos_clos_90A3	2	cyclic-lactone-autoinducer, ranthipeptide
GCF_000371585.1_Clos_clos_90A3_V	2	cyclic-lactone-autoinducer, ranthipeptide
GCF_000424325.1_ASM42432v1	2	cyclic-lactone-autoinducer, ranthipeptide
GCF_001078445.1_Clos_clos_WAL_7855_v11	2	ranthipeptide, NRPS-like
GCF_003467855.1_ASM346785v1	2	ranthipeptide, NRPS-like
GCF_900100685.1_IMG-taxon_2654588145	2	ranthipeptide, NRPS-like
GCF_902374585.1_MGYG-HGUT-01386	2	cyclic-lactone-autoinducer, ranthipeptide
GCF_900100685.1	2	cyclic-lactone-autoinducer, ranthipeptide
GCF_900108895.1_IMG-taxon_2654588144	2	cyclic-lactone-autoinducer, ranthipeptide
GCF_900447015.1_57530_A01	2	ranthipeptide, NRPS-like
GCF_000371485.1_Clos_clos_90B1_V1	2	cyclic-lactone-autoinducer, ranthipeptide
GCF_001405335.1_13470_2_84	1	ranthipeptide

GCF_000371525.1_Clos_clos_90A7_V1	1	ranthipeptide
43841.90A7.1_	1	ranthipeptide
43841.C14940.1	1	ranthipeptide
GCF_003433765.1_ASM343376v1	1	ranthipeptide
C. symbiosum		
GCA_902652275.1_CsymbiosumLFYP84	2	ranthipeptide, NRPS
GCF_000189595.1_Clos_symb_WAL_14163_V1	1	ranthipeptide
GCF_000189615.1_Clos_symb_WAL_14673_V2	1	ranthipeptide
52421E_LM19B	1	ranthipeptide
52422E_LM19R	1	ranthipeptide
GCF_003463485.1_ASM346348v1	1	ranthipeptide
GCF_001406475.1_13470_2_83_	1	ranthipeptide
GCF_008632235.1_ASM863223v1	1	ranthipeptide
GCF_900049235.1	1	ranthipeptide
GCF_003468225.1_ASM346822v1	1	ranthipeptide
GCF_900461275.1_51765_A02	1	ranthipeptide
GCF_902167935.1_TS_8243C_mod2_	1	ranthipeptide
CF_902374315.1_MGYG-HGUT-01367	1	ranthipeptide
GCF_005845085.1_ASM584508v1	1	ranthipeptide
C. bolteae		
GCF_003464745.1_ASM346474v1	3	cyclic-lactone-autoinducer, rantipeptide, NRPS-like
GCA_004555815.1_ASM455581v1	3	phosphonate, NRPS-like, ranthipeptide
GCA_004558155.1_ASM455815v1	2	ranthipeptide, cyclic-lactone-autoinducer
GCF_000154365.1_ASM15436v1	2	ranthipeptide, NRPS-like
GCF_000371645.1_Clos_bolt_90B8_V1_	2	ranthipeptide, NRPS-like
GCF_000371665.1_Clos_bolt_90B7_V1	2	ranthipeptide, NRPS-like
GCF_000371725.1_Clos_bolt_90A5_V1	2	ranthipeptide, NRPS-like
GCF_002234575.1_ASM223457v1	2	ranthipeptide, NRPS-like

GCF_002959675.1_ASM295967v1	2	ranthipeptide, NRPS-like
GCF_003439835.1_ASM343983v1	2	ranthipeptide, NRPS-like
GCF_003458165.1_ASM345816v1	2	ranthipeptide, NRPS-like
GCF_003458625.1_ASM345862v1	2	ranthipeptide, NRPS-like
GCF_902375545.1_MGYG-HGUT-01493	2	ranthipeptide, NRPS-like
GCA_902652185.1_CbolteaeLFYP116	1	ranthipeptide
GCF_000371705.1_Clos_bolt_90A9_V1	1	ranthipeptide
GCF_003437595.1_ASM343759v1	1	ranthipeptide

Table 5: Putative secondary metabolite producing regions in *Clostridium* XIV species. antiSMASH analysis indicating that as well as having larger genomes, *C. clostridioforme* strains LM41 and LM42 contain, alongside strain *C. clostridioforme* YL32, increased numbers of BGCs indicating increased capability to make secondary metabolites. While these strains had either 10 or 13 BGCs each the majority of other strains, including *C. symbiosum* LM19B and LM19R carried a single BGC for a putative ranthipeptide.

Supplementary Figures

Supplementary Figure 1: R plots of Roary analysis of *C. clostridioforme.* Roary plots showing the number of; new genes, conserved genes, number of genes in the pan genome, unique genes, BlastP hits with a different percentage, conserved versus total genes, and new versus unique genes when compared across the cluster**.**

Supplementary Figure 2: R plots of Roary analysis of *C. symbiosum.* Roary plots showing the number of; new genes, conserved genes, number of genes in the pan genome, unique genes, BlastP hits with a different percentage, conserved versus total genes, and new versus unique genes when compared across the cluster**.**

Supplementary Figure 3: R plots of Roary analysis of *C. bolteae.* Roary plots showing the number of; new genes, conserved genes, number of genes in the pan genome, unique genes, BlastP hits with a different percentage, conserved versus total genes, and new versus unique genes when compared across the cluster**.**

Supplementary Table 1

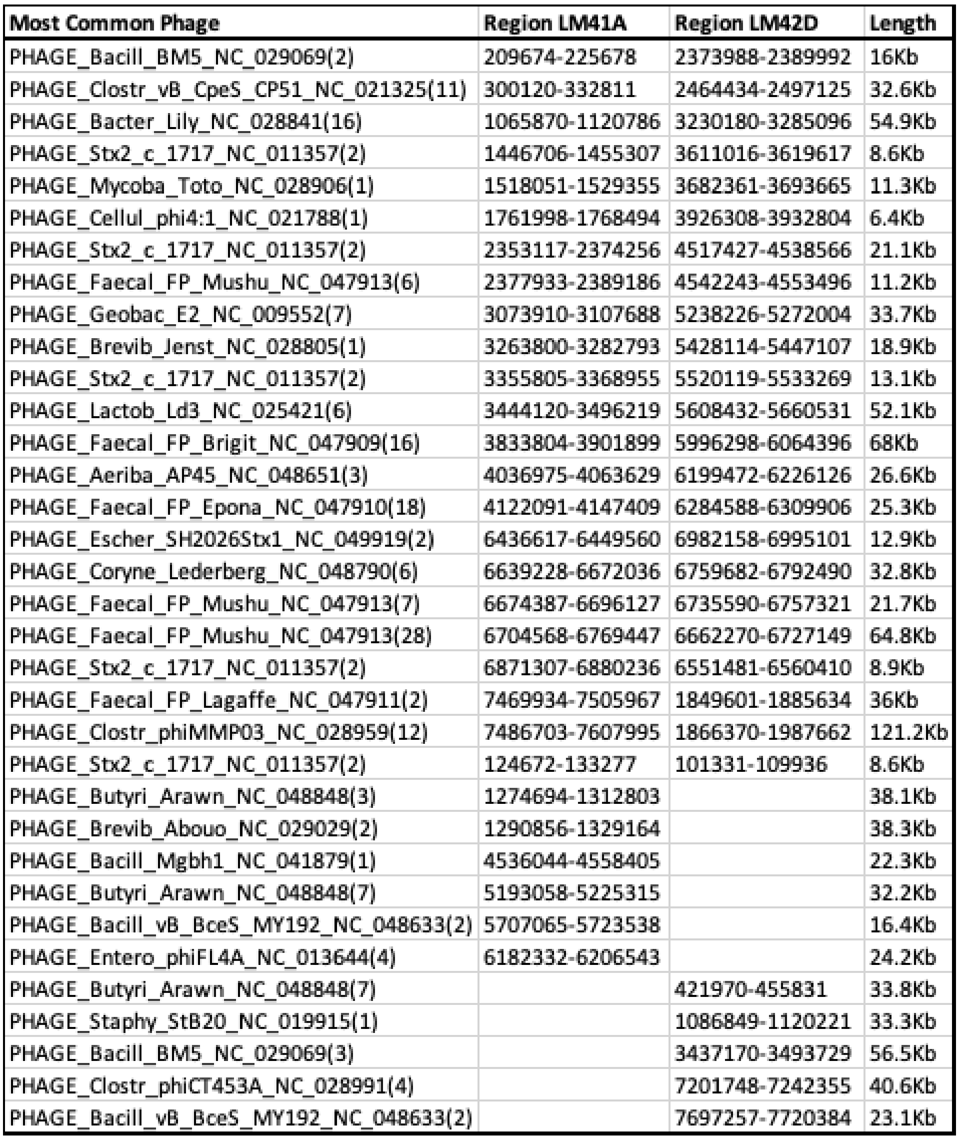

Most Common Phage	Region LM41A	Region LM42D	Length
PHAGE_Bacill_BM5_NC_029069(2)	209674-225678	2373988-2389992	16Kb
PHAGE_Clostr_vB_CpeS_CP51_NC_021325(11)	300120-332811	2464434-2497125	32.6Kb
PHAGE_Bacter_Lily_NC_028841(16)	1065870-1120786	3230180-3285096	54.9Kb
PHAGE_Stx2_c_1717_NC_011357(2)	1446706-1455307	3611016-3619617	8.6Kb
PHAGE_Mycoba_Toto_NC_028906(1)	1518051-1529355	3682361-3693665	11.3Kb
PHAGE_Cellul_phi4:1_NC_021788(1)	1761998-1768494	3926308-3932804	6.4Kb
PHAGE_Stx2_c_1717_NC_011357(2)	2353117-2374256	4517427-4538566	21.1Kb
PHAGE_Faecal_FP_Mushu_NC_047913(6)	2377933-2389186	4542243-4553496	11.2Kb
PHAGE_Geobac_E2_NC_009552(7)	3073910-3107688	5238226-5272004	33.7Kb
PHAGE_Brevib_Jenst_NC_028805(1)	3263800-3282793	5428114-5447107	18.9Kb
PHAGE_Stx2_c_1717_NC_011357(2)	3355805-3368955	5520119-5533269	13.1Kb
PHAGE_Lactob_Ld3_NC_025421(6)	3444120-3496219	5608432-5660531	52.1Kb
PHAGE_Faecal_FP_Brigit_NC_047909(16)	3833804-3901899	5996298-6064396	68Kb
PHAGE_Aeriba_AP45_NC_048651(3)	4036975-4063629	6199472-6226126	26.6Kb
PHAGE_Faecal_FP_Epona_NC_047910(18)	4122091-4147409	6284588-6309906	25.3Kb
PHAGE_Escher_SH2026Stx1_NC_049919(2)	6436617-6449560	6982158-6995101	12.9Kb
PHAGE_Coryne_Lederberg_NC_048790(6)	6639228-6672036	6759682-6792490	32.8Kb
PHAGE_Faecal_FP_Mushu_NC_047913(7)	6674387-6696127	6735590-6757321	21.7Kb
PHAGE_Faecal_FP_Mushu_NC_047913(28)	6704568-6769447	6662270-6727149	64.8Kb
PHAGE_Stx2_c_1717_NC_011357(2)	6871307-6880236	6551481-6560410	8.9Kb
PHAGE_Faecal_FP_Lagaffe_NC_047911(2)	7469934-7505967	1849601-1885634	36Kb
PHAGE_Clostr_phiMMP03_NC_028959(12)	7486703-7607995	1866370-1987662	121.2Kb
PHAGE_Stx2_c_1717_NC_011357(2)	124672-133277	101331-109936	8.6Kb
PHAGE_Butyri_Arawn_NC_048848(3)	1274694-1312803		38.1Kb
PHAGE_Brevib_Abouo_NC_029029(2)	1290856-1329164		38.3Kb
PHAGE_Bacill_Mgbh1_NC_041879(1)	4536044-4558405		22.3Kb
PHAGE_Butyri_Arawn_NC_048848(7)	5193058-5225315		32.2Kb
PHAGE_Bacill_vB_BceS_MY192_NC_048633(2)	5707065-5723538		16.4Kb
PHAGE_Entero_phiFL4A_NC_013644(4)	6182332-6206543		24.2Kb
PHAGE_Butyri_Arawn_NC_048848(7)		421970-455831	33.8Kb
PHAGE_Staphy_StB20_NC_019915(1)		1086849-1120221	33.3Kb
PHAGE_Bacill_BM5_NC_029069(3)		3437170-3493729	56.5Kb
PHAGE_Clostr_phiCT453A_NC_028991(4)		7201748-7242355	40.6Kb
PHAGE_Bacill_vB_BceS_MY192_NC_048633(2)		7697257-7720384	23.1Kb

Supplementary Table 1: Phage carriage by *C. clostridioforme* strains LM41 and LM42. Analysis of phage carriage by Phaster of *C. clostridioforme* strains LM41 and LM42 indicated while many phage regions were common to both strains, each had 5-6 putative phage regions absent in the other strain.